WILEY

Frontiers in Flow Cytometry™

24 hour Virtual Event

September 13th, 2023

Frontiers in Flow Cytometry™ is for researchers across the globe looking for an opportunity to share and learn about current developments in flow cytometry. This 24 hour virtual event will feature keynote presentations by industry colleagues, webinars, demos, live networking opportunities and more.

Key topics include:

- Spectral and conventional flow cytometry
- Immunophenotyping and Standardization
- Panel design and optimization
- Cancer Biology and Auto-immune Diseases
- Infectious diseases
- Advances in flow cytometry technology

Register Now

This event is sponsored by ThermoFisher SCIENTIFIC

Specific Localization and Quantification of the Oligo-Mouse-Microbiota (OMM^{12}) by Fluorescence *In Situ* Hybridization (FISH)

Sandrine Brugiroux,[1,2] David Berry,[3] Diana Ring,[1] Nicolas Barnich,[2] Holger Daims,[3] and Bärbel Stecher[1,4,5]

[1]Max von Pettenkofer Institute, LMU Munich, Munich, Germany
[2]M2iSH, UMR 1071 Inserm, University of Clermont Auvergne, Clermont-Ferrand, France
[3]Centre for Microbiology and Environmental Systems Science, Division of Microbial Ecology, University of Vienna, Vienna, Austria
[4]German Center for Infection Research, Partner Site Munich, Germany
[5]Corresponding author: *stecher@mvp.lmu.de*

Published in the Microbiology section

The oligo-mouse-microbiota (OMM^{12}) is a widely used syncom that colonizes gnotobiotic mice in a stable manner. It provides several fundamental functions to its murine host, including colonization resistance against enteric pathogens. Here, we designed and validated specific fluorescence *in situ* hybridization (FISH) probes to detect and quantify OMM^{12} strains on intestinal tissue cross sections. 16S rRNA–specific probes were designed, and specificity was validated on fixed pure cultures. A hybridization protocol was optimized for sensitive detection of the individual bacterial cells in cryosections. Using this method, we showed that the intestinal mucosal niche of *Akkermansia muciniphila* can be influenced by global gut microbial community context. © 2022 The Authors. Current Protocols published by Wiley Periodicals LLC.

Basic Protocol: Localization and quantification of OMM^{12} single strains in mouse cecum cross section
Support Protocol: Establishment of specific FISH probe set for OMM^{12} syncom

Keywords: altered Schaedler flora • intestine • microbial ecology • oligo-MM • sDMDMm2 • single-cell analysis • spatial structure

How to cite this article:
Brugiroux, S., Berry, D., Ring, D., Barnich, N., Daims, H., & Stecher, B. (2022). Specific localization and quantification of the oligo-mouse-microbiota (OMM^{12}) by fluorescence *in situ* hybridization (FISH). *Current Protocols*, *2,* e548. doi: 10.1002/cpz1.548

INTRODUCTION

Mammalian gut microbial communities harbor bacteria, archaea, viruses, protists, and fungi. Bacterial communities, maintaining a mutualistic relationship with their host, confer numerous health benefits ranging from breakdown of dietary components to metabolite production and maturation of immune functions (Lozupone, Stombaugh, Gordon,

CURRENT PROTOCOLS
A Wiley Brand

Current Protocols e548, Volume 2
Published in Wiley Online Library (wileyonlinelibrary.com).
doi: 10.1002/cpz1.548

Jansson, & Knight, 2012). Consequently, the risk for common human diseases has been associated with altered intestinal bacterial profiles (Ebrahimzadeh Leylabadlo, Sanaie, Sadeghpour Heravi, Ahmadian, & Ghotaslou, 2020; Moszak, Szulińska, & Bogdański, 2020; Nagao-Kitamoto & Kamada, 2017; Zhao, Zhang, Zuo, & Yu, 2017). Bulk community profiling has given valuable insight into the development and dynamics of the gastrointestinal microbiome (Bäckhed et al., 2015; Faith et al., 2013; Falony et al., 2016). However, there are many lines of evidence that spatial organization of the bacterial community along not only the longitudinal but also the lateral axis is important for its functionality. Spatial structure of the community can be altered during diseases (Desai et al., 2016; Stecher et al., 2008; Swidsinski, Loening-Baucke, Vaneechoutte, & Doerffel, 2008) in response to diet (Riva et al., 2019; Tropini, Earle, Huang, & Sonnenburg, 2017) or in immunodeficiency (Blum et al., 2020; Nakajima et al., 2018). To decipher how microbial biogeography is linked to its functions and provide more insight into the functionally relevant interactions, microscopy-based methods are essential. The most common method, which does not depend on genetic modification of the bacteria, is fluorescence *in situ* hybridization (FISH) using species- or group-specific fluorescently labeled 16S rRNA gene–targeted probes (Daims, Stoecker, & Wagner, 2005).

Research using synthetic microbial communities has gained popularity in recent years, and gnotobiotic animals have become essential tools in microbiome research (Clavel, Lagkouvardos, Blaut, & Stecher, 2016; Elzinga, van der Oost, de Vos, & Smidt, 2019; Macpherson & McCoy, 2015). The oligo-mouse-microbiota (OMM^{12}) is composed of 12 phylogenetically diverse bacteria from the murine microbiota (Brugiroux et al., 2016). This model is unique because it exhibits long-term stability in gnotobiotic mice (Brugiroux et al., 2016) and can be reproducibly established in different germ-free facilities (Eberl et al., 2020). Importantly, it recapitulates central physiologic and functional traits of a complex mouse microbiome, including colonization resistance to enteric pathogens (Brugiroux et al., 2016; Studer et al., 2016). The genomes of the 12 bacterial strains have been sequenced (Garzetti et al., 2017), and strains are publicly available from the German Type Culture Collection (DSMZ) for noncommercial use. Hence, the OMM^{12} is widely distributed and currently used by over 40 research groups worldwide to decipher molecular interactions between host and gut microbiota under health and disease (Bolsega et al., 2019; Brugiroux et al., 2016; Eberl et al., 2020; Fischer et al., 2020; Herp et al., 2019; Kuczma et al., 2020; Li et al., 2015; Lourenço et al., 2020; Marion et al., 2020; Studer et al., 2016; van Tilburg Bernardes et al., 2020; Wotzka et al., 2019; Wyss et al., 2020). Spatial analysis of the OMM^{12} using strain-specific FISH probes, in combination with stable isotope-labeling approaches and downstream *in vitro* characterization of the strains, will allow deep insight into how interspecies and host-microbe interactions shape essential functions of this widely used synthetic community (Pereira et al., 2020).

Therefore, we developed a strain-specific probe set for FISH-based spatial analysis of the OMM^{12}, a synthetic bacterial community. Here we present a protocol to specifically identify and quantify the individual OMM^{12} bacteria *in situ* in intestinal cross sections. Furthermore, we provide a protocol used to design and validate FISH probes, as well as to optimize fluorescence signal intensity.

STRATEGIC PLANNING

Essentially, FISH probes need to be developed for each of the target bacteria that will be specifically studied. For the OMM community, probes are already identified (Table 1), but this protocol can be expanded to target any specific taxa of interest. For designing specific probes, please refer to the Support Protocol. Further, the power of this technique is to capture differences in the quantity, distribution, and physical interaction of the various taxa under different *in vivo* conditions such as infection and dietary changes.

Table 1 OMM[12]-Targeted FISH Probes

Designation	Sequence (5′ to 3′)	Strain specificity	Tested fluorophores	Optimal [FA], %	Reference
YL2_180	CACCATGCGGTGGGGCGGAGCA	*Bifidobacterium animalis* YL2	2 × Cy3	20	This article
YL27_180	AGATGCCTCCCCTCGGCCACA	*Muribaculum intestinale* YL27	2 × Cy3 or 2 × FITC	30	This article
YL31_180	CCATGCGACCCAACTGCATCA	*Flavonifractor plautii* YL31	2 × Cy3	35	This article
YL32_180	CCATGCGGCACTGTGCGCTTA	*Enterocloster clostridioformis* YL32	2 × Cy3 or 2 × FITC	30	This article
Muc1437	CCTTGCGGTTGGCTTCAGAT	*Akkermansia muciniphila* YL44	2 × Cy3 or 2 × FITC	30	Derrien et al. (2008)
BET940	TTAATCCACATCATCCACCG	*Turicimonas muris* YL45	2 × Cy3	30	Demanèche et al. (2008)
YL58_180	CCATGCAGCCCTGTGCGCTTA	*Blautia coccoides* YL58	2 × FITC	30	This article
I46_180	AGTATGCGCTCTGTATACCTA	*Clostridium innocuum* I46	2 × Cy3	30	This article
I48_180	TCATGCGATCTTGATATCCTA	*Bacteroides caecimuris* I48	2 × Cy3 or 2 × FITC	30	This article
I49_180	GCCATGTGGCTTTTGTTGTTA	*Limosilactobacillus reuteri* I49	2 × Cy3 or 2 × FITC	30	This article
KB1_180	GCCATGCGGCATAAACTGTTA	*Enterococcus faecalis* KB1	2 × Cy3	30	This article
KB18_180	CCATGCGATAAGATAATGTCA	*Acutalibacter muris* KB18	2 × Cy3	n.d.	This article
EUB338 I	GCT GCC TCC CGT AGG AGT	Most bacteria	–	–	Amann et al. (1990)
EUB338 III	GCT GCC ACC CGT AGG TGT	*Verrucomicrobiales*	–	–	Daims et al. (1999)

Cy3, cyanine 3; [FA], formamide concentration; FISH, fluorescence *in situ* hybridization; FITC, fluorescein isothiocyanate; n.d., not determined; OMM[12], oligo-mouse-microbiota.
Designations of FISH probes designed in this study were followed by the starting position (e.g., xxx_180) of the probe when aligned to the 16S rRNA gene of *Escherichia coli*.

LOCALIZATION AND QUANTIFICATION OF OMM[12] SINGLE STRAINS IN MOUSE CECUM CROSS SECTION

This protocol presents a method to fix mouse gut tissue before cryosectioning, then to fluorescently label each single OMM[12] strain on mouse tissue, and finally to localize and quantify each OMM[12] strain *in vivo*.

Materials

Mouse of interest
4% (w/v) paraformaldehyde (PFA; see recipe)
20% (w/v) sucrose in phosphate-buffered saline (PBS)
Tissue-Tek Optimal Cutting Temperature (O.C.T.) compound
Liquid nitrogen
50%, 80%, and 96% ethanol
Hybridization buffers (see Table 2)
Nail varnish
FISH probe (see Support Protocol)
Washing buffers (see Table 3)
Antifade mounting medium (e.g., Vectashield)

Dental floss
Surgical scissors
2.5-ml sample cup with snap-in lid, 32 × 14 mm (e.g., A. Hartenstein, cat. no. PR02)
Cryotome (e.g., Leica CM1950)
Superfrost Plus slides, 75 × 25 × 1 mm (e.g., A. Hartenstein, cat. no. OTS)
2-ml microcentrifuge tubes
Vortex mixer
50-ml conical tubes
Absorbent paper
Variable temperature oven, dry heat, protected from light
Confocal microscope (e.g., Leica TCS SP5) with image acquisition software
Digital Image Analysis in Microbial Ecology (DAIME) software, version 2.2 (available at: *https://dome.csb.univie.ac.at/daime*; Daims, Lücker, & Wagner, 2006)

Additional reagents and equipment for mouse euthanasia (see *Current Protocols* article: Donovan & Brown, 2005)

NOTE: All protocols involving live animals must be reviewed and approved by the appropriate animal care and use committee and must follow regulations for the care and use of laboratory animals.

Preparation and fixation of mouse gut tissue in 4% paraformaldehyde

1. Sacrifice mouse by opening the abdomen and carefully exposing intestinal organs (e.g., cecum) without squeezing the organs.
2. Use dental floss to close intestinal parts of interest with a node, and excise it (e.g., 1 cm cecum tip).
3. Fix closed organ in 2 ml ice-cold 4% (w/v) PFA in 2.5-ml sample cups with snap-in lid at 4°C overnight.
4. The next morning, discard 4% (w/v) PFA, and replace with 20% (w/v) sucrose in PBS. Incubate overnight at 4°C.

Table 2 Composition of Hybridization Buffers[a]

Reagent	Volume (μl)												
Formamide (% final)	0	5	10	15	20	25	30	35	40	45	50	55	70
5 M NaCl	180	180	180	180	180	180	180	180	180	180	180	180	180
1 M Tris•HCl	20	20	20	20	20	20	20	20	20	20	20	20	20
Deionized distilled water	799	749	699	649	599	549	499	449	399	349	299	249	99
Formamide	0	50	100	150	200	250	300	350	400	450	500	550	700
10% SDS[b]	1	1	1	1	1	1	1	1	1	1	1	1	1

SDS, sodium dodecyl sulfate.
[a] Buffers should be prepared in tightly closable 2-ml tubes and, preparation should be conducted in a fume hood as formamide is highly toxic and volatile.
[b] SDS should be added inside the lid of the 2-ml tube, which will be vortexed immediately before use.

5. Remove 20% (w/v) sucrose in PBS, and dab organ on paper tissue to remove excess liquid.
6. Embed tissue vertically in O.C.T. compound until it is covered (1 to 2 ml), and snap freeze in liquid nitrogen.
7. Store frozen samples at −80°C.
8. Generate 7-μm thick cryosections from region of interest (ROI) using a cryotome, and air-dry sections on superfrost plus slides at least one night before hybridization at room temperature.

Fluorescence in situ hybridization of mouse gut sections

In order to increase fluorescence signal, FISH probes can be double labeled at 3' and 5' ends. This trick was previously described by Stoecker, Dorninger, Daims, & Wagner (2010). In our case, probes were double labeled with either fluorescein isothiocyanate (FITC), cyanine 3 (Cy3), or Cy5 and then purified by high-performance liquid chromatography (HPLC) and lyophilized by commercial suppliers. Antisense probes should be used as negative controls. Bacterial DNA can be stained by Sytox-Green.

9. Dehydrate gut sections using increasing concentrations of ethanol (50%, 80%, and 96%) for 3 min each.
10. Air dry ∼5 min. Meanwhile, prepare all hybridization buffers (see Table 2) at 0%, 10%, 20%, 30%, 35%, 40%, 45%, and 55% formamide in a fume hood. Prepare one 2-ml tube per FISH probe. Be careful to add sodium dodecyl sulfate (SDS) inside the lid of the 2-ml tube, and vigorously vortex right before use.
11. Deposit nail varnish around each dehydrated section mounted on the superfrost plus slide to build a barrier that keeps liquid on the section.
12. Prepare one moist chamber per slide: take one 50-ml tube, and insert a piece of absorbent paper at the bottom.
13. Depending on the amount of sections, take an aliquot of the freshly prepared hybridization buffer out of the 2-ml tube, and mix with FISH probe at a final concentration of 5 ng/μl. Use 50 to 100 μl per section (depending on section size).
14. Pour remaining hybridization buffer from the 2-ml tube into the moist chamber to humidify it.
15. Incubate slide within the horizontally oriented, closed, moist chamber for 4 hr at 46°C in the dark. Meanwhile, prepare corresponding washing buffer (see Table 3) in

Table 3 Composition of Washing Buffers[a]

Reagent	Volume (ml)												
Formamide (%)[b]	0	5	10	15	20	25	30	35	40	45	50	55	70
5 M NaCl	9.0	6.3	4.5	3.2	2.2	1.5	1.0	0.7	0.5	0.3	0.2	0.1	0
1 M Tris•HCl	1	1	1	1	1	1	1	1	1	1	1	1	1
0.5 M EDTA	0	0	0	0	0.5	0.5	0.5	0.5	0.5	0.5	0.5	0.5	0.5

[a] After addition of reagents, all solutions should be brought to 50 ml using deionized distilled water.
[b] Indicates the formamide concentration in the corresponding hybridization buffer.

50-ml tubes using the same formamide concentration as in the hybridization buffers. Prewarm tubes containing washing buffer at 48°C.

16. Mix tube containing washing buffer by inversion.
17. Quickly place slide into tube containing washing buffer in a fume hood, and incubate slide 10 min at 48°C.
18. Rinse slide 5 s in ice-cold distilled water to avoid nonspecific probe binding.
19. Dry slide in a laminar flow hood in the dark for 5 to 10 min until dry.
20. Mount slide in the dark using antifade mounting medium. To do so, add a drop of mounting medium to each section, and then add a coverslip. Seal with nail varnish, and dry and store in the dark at 4°C before analysis.

Image acquisition and fluorescence signal analysis

21. Acquire TIFF images (1024 × 1024) using a confocal microscope within 24 hr.

    In our case, TIFF images were obtained using Leica LAS AF software.

22. Import merge and grayscale images in .tif format into DAIME software.

    *Be careful to properly label images; for example, label as **X_#** where **X** is common to all images (letters or number only) and **#** is the image number. Moreover, images from different channels (including merge) must be in a separate file.*

23. Set up image scale by clicking on the "ruler" icon.

    The z-scale corresponds to the number of images.

24. Open the visualizer option, and click on the "OBJ" icon, then on "2D segmentation."
25. Click on the "freehand" icon, and left click to draw a line to define the ROI. Then, close ROI using a right click.
26. Convert ROI to an object using the corresponding icon.
27. Sequentially click "Analysis," "Biofilm tool," and "Create Slicer template…," and enter desired slice thickness. Select appropriated slicing direction, and then press OK.

    The baseline smoothing is 19% by default. Smoothing represents how precisely the slice bands are going to follow the epithelial borderline.

28. Open resulting object series in visualizer, and click the "OBJ" icon. Click the "rainbow" button to better visualize the different slices, and save file as .stk format.

    If needed, a single slice can be rejected from the analysis. Right click on the slice, and then reject it as a normal object. It can also be rejected in the selected image or in all of them (tick "in all images" option).

29. Manually check each gray level picture to remove background particles that could bias analysis. To do so, select a gray level channel. Open visualizer and use the "OBJ" icon. After having deleted an object, perform a new 2D segmentation.

    Nutrients and other gut contents emit autofluorescence such as in Cy3 and FITC channels. Deletion of autofluorescent particles is feasible using the "Image Calculator" icon to subtract the Cy3 channel from the FITC channel.

30. Sequentially click "Analysis," "Biofilm tools," and then "Slice & quantify biovolume fraction" to quantify relative biovolume using the robust automated threshold selection (RATS) algorithm (Kittler, Illingworth, & Föglein, 1985). Ignore objects up to five pixels (Daims & Wagner, 2007).

    The user should not consider the analysis results as good under 80% congruency (i.e., 80% of the targeted population only also stained with the Eub probes).

31. Export and save the final data.

    As an example, saved files can be opened under Editor, and then copied and pasted into spreadsheet analysis software.

    The orange icon "LOG" allows the user to see the commands history, which can also be exported as HTML or plain text.

    An example of the result is presented in Understanding Results.

ESTABLISHMENT OF SPECIFIC FISH PROBE SET FOR OMM^{12} SYNCOM

SUPPORT PROTOCOL

To establish an OMM^{12} FISH probe set, probes were designed using ARB software. In order to validate FISH probe strain specificity and optimize fluorescence signal intensity, pure OMM^{12} bacterial cultures were anaerobically grown, fixed in PFA, and then stored at −20°C. Determination of optimal formamide concentration, and thus optimal hybridization stringency, was achieved by performing FISH using gradients of formamide concentrations on each probe-strain combination. Finally, probe strain specificity was confirmed using pure fixed OMM^{12} bacterial suspensions. Such an approach can be used to validate other FISH probes.

Additional Materials *(also see Basic Protocol)*

OMM^{12} strain of interest
Brain heart infusion medium (see recipe)
Anaerobic *Akkermansia* medium (see recipe)
Anaerobic gas mixture (7% H_2, 10% CO_2, 83% N_2)
PBS

ARB software (available at: *http://www.arb-home.de*)
Anaerobic cultivation platform (e.g., Coylab Anerobic Chamber)
Spectrophotometer
Centrifuge
10-well diagnostic slides, 76 × 25 × 1 mm (e.g., Thermo Fisher Scientific)

Additional reagents and equipment to perform culture using the Hungate technique (for detailed description see *https://www.dsmz.de/fileadmin/Bereiche/Microbiology/Dateien/Kultivierungshinweise/englAnaerob.pdf*)

Fluorescence in situ hybridization probe design

1. Load full-length 16S rRNA gene sequences of all OMM^{12} bacterial strains into ARB, and use SILVA SSU NR database as described in Ludwig et al. (2004) and Quast et al. (2013). See Table 1 for probe sequences and further information.

Preparation of bacterial anaerobic cultures

2. Inoculate one stock of each OMM^{12} strain either in 10 ml brain heart infusion medium for strict anaerobes or in 10 ml anaerobic *Akkermansia* medium for *A. muciniphila* YL44 (Derrien, Vaughan, Plugge, & de Vos, 2004). Incubate at 37°C without agitation in anaerobic cultivation platform. After 24 hr prepare subcultures: 200 µl culture in 10 ml fresh medium.
3. Gas first and subcultures using the Hungate technique and an anaerobic gas mixture (7% H_2, 10% CO_2, 83% N_2).
4. Incubate subculture at 37°C until the optical density at 600 nm (OD_{600}) = 1, which depending on the growth rate can take several hours to days.

   As an exception, YL45 is translucent and will not reach $OD_{600} = 1$.

   Anaerobic cultivation of the OMM^{12} strains is also described in Brugiroux et al. (2016).

Fixation of bacterial culture in 4% paraformaldehyde

5. Centrifuge 250 µl of each culture (250 µl YL45 after 48 hr subculture) in a 2-ml tube 5 min at 6800 × *g*, 4°C.
6. Discard supernatant and resuspend pellet in 750 µl ice-cold 4% (w/v) PFA.
7. Incubate 3 hr at 4°C.
8. Centrifuge 5 min at 6800 × *g*, 4°C.
9. Discard supernatant and resuspend pellet in 1 ml ice-cold PBS.
10. Wash three times in ice-cold PBS, centrifuging 5 min at 10,600 × *g*, 4°C, between each step.
11. Resuspend bacterial pellet in 250 µl ice-cold PBS and 250 µl ice-cold 96% ethanol.
12. Store at −20°C before use.

Optimization of hybridization stringency

In order to increase fluorescence signal, FISH probes can be double labeled at 3' and 5' ends. This trick was previously described by Stoecker et al. (2010). In our case, probes were double labeled with either FITC, Cy3, or Cy5 and then purified by HPLC and lyophilized by commercial suppliers. To identify the optimal formamide concentration for each probe, increasing formamide concentrations (0%, 10%, 20%, 30%, 35%, 40%, 45%, and 55%) are tested for maximal signal strength and specificity.

13. After probe synthesis, resuspend probes in distilled water to generate 100 ng/µl stock solutions and to later prepare 50 ng/µl working solutions. Store all probes at −20°C.
14. Spot 2 µl/well PFA-fixed bacterial suspension onto diagnostic slides, and dry at 46°C for 5 min.
15. Incubate slide sequentially in 50% ethanol, 80% ethanol, and then 96% ethanol for 3 min each.
16. Air dry for about 5 to 10 min. Meanwhile, prepare all hybridization buffers (see Table 2) at 0%, 10%, 20%, 30%, 35%, 40%, 45%, and 55% formamide in a fume hood. Prepare one 2-ml tube per FISH probe. Be careful to add SDS inside the lid of the 2-ml tube, and vigorously vortex it right before use.
17. Prepare one moist chamber per slide: take one 50-ml tube, and insert a piece of absorbent paper at the bottom.

18. Depending on the amount of spots, take an aliquot of the freshly prepared hybridization buffer out of the 2-ml tube, and mix with FISH probe at a final concentration of 5 ng/µl. Use 20 µl per spot.
19. Pour remaining hybridization buffer from the 2-ml tube into the moist chamber to humidify it. Incubate diagnostic slide within the horizontally oriented, closed, moist chamber for 4 hr at 46°C in the dark. Meanwhile, prepare corresponding washing buffer (see Table 3) in 50-ml tubes, using the same formamide concentration as in the hybridization buffers. Prewarm tubes containing washing buffer at 48°C.
20. Mix tube containing washing buffer by inversion.
21. Quickly place diagnostic slide into tube containing washing buffer in a fume hood, and incubate slide 10 min at 48°C.
22. Rinse slide 5 s in ice-cold distilled water to avoid nonspecific probe binding.
23. Dry slide in a laminar flow hood in the dark for 5 to 10 min until dry.
24. Mount slide in the dark using antifade mounting medium. To do so, add a drop of mounting medium to each spot, and then add a coverslip. Seal with nail varnish, and dry and store in the dark at 4°C before analysis.

Image acquisition and fluorescence signal analysis

25. Acquire TIFF images (1024 × 1024) using a confocal microscope within 24 hr.

    In our case, TIFF images were obtained using Leica LAS AF software.

26. Import TIFF images as .tif format into DAIME software.

    *Be careful to properly label TIFF images; for example, label as **f%-#** where **%** corresponds to the tested formamide concentration (number only) and **#** is the image number.*

27. Open the visualizer option, and click on the "OBJ" icon and then on "2D segmentation" using the RATS algorithm (Kittler et al., 1985). Ignore objects up to five pixels (Daims & Wagner, 2007).
28. Click the "FA%" icon.
29. Export "Mean for each FA conc.," and use these data for plotting.

REAGENTS AND SOLUTIONS

Anaerobic Akkermansia medium

1. To distilled water, add 18.5 g/L brain heart infusion (e.g., Oxoid, cat. no. CM1135), 15 g/L trypticase soy broth (e.g., Oxoid, cat. no. CM0129), 5 g/L yeast extract (e.g., Carl Roth, cat. no. 2363.3), 2.5 g/L K_2HPO_4 (e.g., Carl Roth, cat. no. P749.1), 1 mg/L hemin (e.g., Sigma-Aldrich, cat. no. 51280), and 0.5 g/L D-glucose (e.g., Carl Roth, cat. no. HN06.2).
2. Sterilize by autoclaving.
3. Under sterile conditions, add 0.5 mg/L menadione (e.g., Sigma-Aldrich, cat. no. M5625), 3% (v/v) heat-inactivated fetal calf serum, 0.25 g/L hog gastric mucin (e.g., Sigma-Aldrich, cat. no. M1778), 0.5 g/L cysteine-HCl•H_2O (e.g., Sigma-Aldrich, cat. no. C7880), and 0.4 g/L Na_2CO_3 (e.g., Merck, cat. no. 106392).
4. Stir for 2 days under anoxic conditions before use to reduce the solution and remove oxygen.
5. Store at room temperature under anaerobic conditions for up to 1 week.

All reagents are dissolved in distilled water except for the hemin, which is resuspended in reagent-grade ethanol supplemented with NaOH until it is entirely dissolved.

Menadione (which is resuspended in reagent-grade ethanol), Na_2CO_3, cysteine-HCl•H_2O, and hog gastric mucin should be sterilized by autoclaving, whereas heat-inactivated fetal calf serum should be filter sterilized.

A. muciniphila YL44 can be grown in this medium, as previously described by Derrien et al. (2004).

Brain heart infusion medium

Distilled water
37 g/L brain heart infusion (e.g., Oxoid, cat. no. CM1135)
0.25 g/L cysteine-HCl•H_2O (e.g., Sigma-Aldrich, cat. no. C7880)
0.25 g/L Na_2S•$9H_2O$ (e.g., Sigma-Aldrich, cat. no. 208043)
Store at room temperature under anaerobic conditions for up to 1 week

Autoclave brain heart infusion after dissolving in distilled water. Then add the remaining reagents under sterile, anoxic conditions.

Prepare cysteine and Na_2S in distilled water, and filter sterilize before storing under anoxic conditions.

Prepare Na_2S in a fume hood because it is highly toxic.

This recipe was obtained from the DSMZ list of media for microorganisms (recipe 215c; available at: https://www.dsmz.de/collection/catalogue/microorganisms/culture-technology/list-of-media-for-microorganisms), which represents a useful tool to gain insight into cultivation conditions and medium recipes.

PFA, 4%

1. Heat 60 ml distilled water to 60°C.
2. Add 8 g PFA and 20 µl of 1 M NaOH.
3. Stir vigorously until PFA is dissolved.
4. Add 20 ml PBS, and bring volume to 200 ml with distilled water.
5. Adjust pH to ∼7.
6. Filter sterilize using a 0.22-µm filter, and aliquot in sterile 50-ml tubes.
7. Store at −20°C for long-term storage.

COMMENTARY

Background Information

In previous studies, we have used FISH approaches to detect and localize targeted bacterial populations (Brugiroux et al., 2016; Herp et al., 2019). In fact, automatic image analysis remains challenging due to software limitations, which leads to an underexploitation of FISH associated data. Here, we present an approach to quantitatively determine bacterial abundance using microscope images, as well as to analyze specific bacterial populations and their enrichment at epithelial borders on gut cross sections of OMM[12] mice.

Critical Parameters

Using this approach, quantification of total and specific bacterial populations is based on biovolume quantification. Therefore, nucleic acid staining such as with DAPI cannot be used to determine total amount of bacteria. This is because the cellular area stained using a nucleic acid stain is too different from the area stained using ribosomal RNA gene–targeted probes.

Optimally, signal intensity of different FISH probes should be similar to each other to optimize image acquisition and analysis. Confocal microscopy is highly recommended, and all images should be generated using the same microscope settings.

Of note, in order to determine whether a bacterial population of interest is enriched at the epithelial border, an ROI must be drawn. Such analysis will only work if the epithelial border is roughly parallel to the picture side.

Troubleshooting

See Table 4 for troubleshooting considerations associated with this protocol.

Understanding Results

A. muciniphila is known to be able to degrade mucin (Derrien et al., 2004). Therefore, we hypothesized that *A. muciniphila* was enriched at the epithelial border. In order to validate our approach, we used the

Table 4 Troubleshooting Guide to Optimize Fluorescent Probe Signal

Problem	Possible cause	Solution
Poor signal	Probe not bound enough to targeted sequence	Increase hybridization time up to 24 hr
		Verify *in silico* that probe sequence is 100% similar to targeted sequence
		Double label FISH probe at 3' and 5' ends
	Fluorophore photobleached	Preserve slides from light as much as possible; use another fluorophore
Unspecific binding	Unspecific binding of fluorophore	Keep slides at 4°C (or at −20°C) before microscope observations

FISH, fluorescence in situ hybridization.

A. muciniphila YL44 strain, which also belongs to the OMM[12] syncom. Three groups of gnotobiotic mice were used: low complexity microbiota (LCM) colonized mice as negative control, LCM mice colonized with YL44 (LCM + YL44), and OMM[12]. YL44 was detected using a Muc1437-Cy3 probe, and total bacterial populations were detected using a Eub338I/III-Cy5 mix. DAPI staining was performed as a control. Confocal images were taken, and merged images were virtually sliced from the epithelial border to the gut lumen (40 μm thick). Then slicer templates were applied to gray level images (Fig. 1D and F). The biovolume of the targeted bacterial population was calculated relative to the biovolume of all bacterial populations. On cecal cross sections of LCM-colonized mice, we observed low Muc1437 signal (Fig. 1A and G). As this signal was not colocalized with Eub338 I/III signal, we concluded that the signal derived from unspecific binding of the probe to the cecal content, which might be due to the fluorophore itself (i.e., Cy3). We confirmed this hypothesis using another fluorophore (FITC), which appeared to exhibit less unspecific binding (data not shown). On cecal sections of LCM + YL44 colonized mice, we observed that the Muc1437 probe hybridized to small coccoid bacterial cells similar to YL44, which seemed to be enriched at the epithelial border (Fig. 1B). When calculating YL44 relative biovolume, we confirmed that YL44 was significantly enriched between 0 and 40 μm from the epithelial border compared to deeper layers within the lumen (Fig. 1H). However, on cecal sections of OMM[12]-colonized mice, YL44 was homogenously distributed in the cecal cross section (Fig. 1C). This was confirmed by the relative biovolume showing no enrichment between 0 and 240 μm from the epithelial border (Fig. 1I).

To sum up, we have established a new approach combining FISH and DAIME analysis in order to specifically detect and quantify a bacterial population through cecal cross sections. We showed that YL44 was enriched at the epithelial border in LCM + YL44–colonized mice but not in OMM[12]-colonized mice. This suggests that the distribution of the YL44 bacterial population in the mouse cecum is dependent on microbial context.

Time Considerations

Staining and analysis of a reasonable number of slides (e.g., 10 to 20) should take ∼2 working days: 1 working day for staining, 0.5 days for image acquisition, and 0.5 days for image analysis using DAIME software.

Acknowledgements

The authors are grateful to the International FISH course attended at the DOME (Division of Microbial Ecology; Vienna, Austria). This work was supported by a BMBF Infektionsgenomik grant. The FISH protocol was adapted from Daims et al. (2005) and Manz, Amann, Ludwig, Wagner, & Schleifer (1992).

Open Access funding enabled and organized by Projekt DEAL.

Author Contributions

Sandrine Brugiroux: conceptualization, data curation, formal analysis, investigation, methodology, resources, validation, visualization, writing—original draft, review, and editing; **David Berry**: formal analysis, investigation, methodology, validation, writing—review and editing; **Diana Ring**: methodology, validation, writing—review and editing; **Nicolas Barnich**: funding acquisition, writing—review and editing; **Holger Daims**: methodology, resources, software, writing—review and editing; **Bärbel Stecher**: conceptualization, funding acquisition, investigation, project administration, resources, supervision, validation, visualization, writing—original draft, review, and editing.

Conflict of Interest

The authors declare no conflicts of interest.

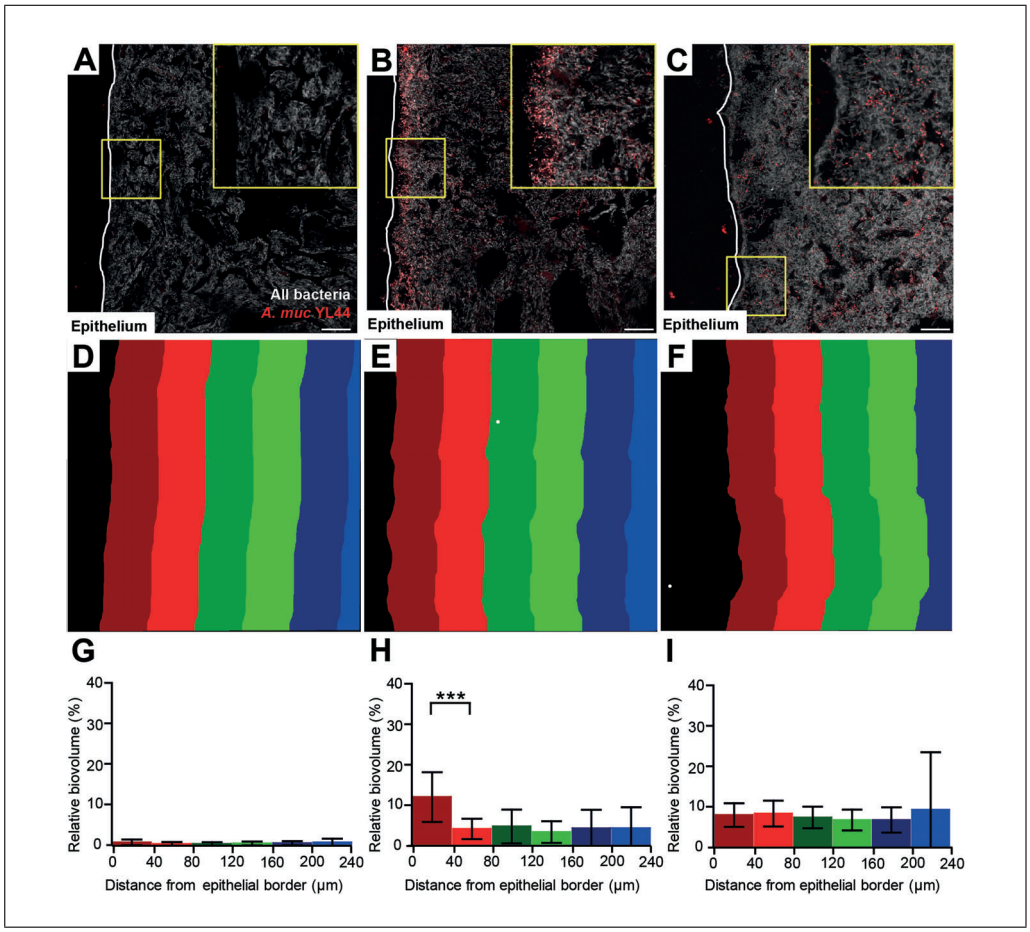

Figure 1 Establishment of a fluorescence *in situ* hybridization (FISH) assay to localize and quantify single strains in the oligo-mouse-microbiota (OMM[12]) mouse gut. Left column: Gnotobiotic mice stably colonized with a low complexity microbiota (LCM; Stecher et al., 2010). Middle column: Gnotobiotic LCM mice inoculated with *Akkermansia muciniphila* YL44 for 21 days (LCM + *A. muc* YL44). Right column: OMM[12] mice stably colonized with 12 strains (*Clostridium innocuum* I46, *Bacteroides caecimuris* I48, *Limosilactobacillus reuteri* I49, *Enterococcus faecalis* KB1, *Bifidobacterium animalis* YL2, *Muribaculum intestinale* YL27, *Flavonifractor plautii* YL31, *Enterocloster clostridioformis* YL32, *A. muciniphila* YL44, *Turicimonas muris* YL45, *Blautia coccoides* YL58, *Acutalibacter muris* KB18). (**A**, **B**, **C**) FISH on paraformaldehyde-fixed cecal cryosections targeting all bacteria (EUB338-I/III, grayscale) and *A. muciniphila* YL44 (Muc1437, red). Upper right squares (yellow) show magnification. Scale bars = 25 µm. White line, epithelial border. (**D**, **E**, **F**) Slicer template generated by DAIME. Same magnification as for A, B, C. Colors represent the different virtual layers from the epithelial border (dark red) to the gut lumen (light blue). Thickness per layer = 40 µm. (**G**, **H**, **I**) *A. muciniphila* YL44 biovolume quantification relative to the EUB338 probe signal using DAIME. (G) LCM-colonized mouse (3 mice, 12 pictures). (H) LCM + *A. muc* YL44-colonized mouse (3 mice, 34 pictures). (I) OMM[12]-colonized mice (5 mice, 33 pictures). Detection limit of YL44 in H and I corresponds to unspecific background fluorescence signal detected in G = 0.65%. Data are given as mean and standard deviation. Mann-Whitney U test: *** $p < .001$. One-way ANOVA Kruskal–Wallis test: (G) $p = .6514$, (H) $p < .0001$, (I) $p = .0643$.

Data Availability Statement

The data, tools, and material (or their source) that support the protocol are available from the corresponding author upon reasonable request.

Literature Cited

Amann, R. I., Binder, B. J., Olson, R. J., Chisholm, S. W., Devereux, R., & Stahl, D. A. (1990). Combination of 16S rRNA-targeted oligonucleotide probes with flow cytometry for analyzing mixed microbial populations. *Applied and Environmental Microbiology*, *56*(6), 1919–1925. doi: 10.1128/aem.56.6.1919-1925.1990

Bäckhed, F., Roswall, J., Peng, Y., Feng, Q., Jia, H., Kovatcheva-Datchary, P., … Jun, W. (2015). Dynamics and stabilization of the human gut microbiome during the first year of life. *Cell Host & Microbe*, *17*(5), 690–703. doi: 10.1016/j.chom.2015.04.004

Blum, F. C., Hardy, B. L., Bishop-Lilly, K. A., Frey, K. G., Hamilton, T., Whitney, J. B., … Mattapallil, J. J. (2020). Microbial dysbiosis during simian immunodeficiency virus infection is partially reverted with combination anti-retroviral therapy. *Scientific Reports*, *10*(1), 6387. doi: 10.1038/s41598-020-63196-0

Bolsega, S., Basic, M., Smoczek, A., Buettner, M., Eberl, C., Ahrens, D., … Bleich, A. (2019). Composition of the intestinal microbiota determines the outcome of virus-triggered colitis in mice. *Frontiers in Immunology*, *10*, 1708. doi: 10.3389/fimmu.2019.01708

Brugiroux, S., Beutler, M., Pfann, C., Garzetti, D., Ruscheweyh, H.-J., Ring, D., … Stecher, B. (2016). Genome-guided design of a defined mouse microbiota that confers colonization resistance against *Salmonella enterica* serovar Typhimurium. *Nature Microbiology*, *2*, 16215. doi: 10.1038/nmicrobiol.2016.215

Clavel, T., Lagkouvardos, I., Blaut, M., & Stecher, B. (2016). The mouse gut microbiome revisited : From complex diversity to model ecosystems. *International Journal of Medical Microbiology*, *306*(5), 316–327. doi: 10.1016/j.ijmm.2016.03.002

Daims, H., Brühl, A., Amann, R., Schleifer, K. H., & Wagner, M. (1999). The domain-specific probe EUB338 is insufficient for the detection of all bacteria: Development and evaluation of a more comprehensive probe set. *Systematic and Applied Microbiology*, *22*(3), 434–444. doi: 10.1016/S0723-2020(99)80053-8

Daims, H., Lücker, S., & Wagner, M. (2006). Daime, a novel image analysis program for microbial ecology and biofilm research. *Environmental Microbiology*, *8*(2), 200–213. doi: 10.1111/j.1462-2920.2005.00880.x

Daims, H., Stoecker, K., & Wagner, M. (2005). Fluorescence in situ hybridization for the detection of prokaryotes. In A. Osborn & C. Smith (Eds.) *Molecular microbial ecology (Advanced methods)* (pp. 213–240). Taylor & Francis.

Daims, H., & Wagner, M. (2007). Quantification of uncultured microorganisms by fluorescence microscopy and digital image analysis. *Applied Microbiology and Biotechnology*, *75*(2), 237–248. doi: 10.1007/s00253-007-0886-z

Demanèche, S., Sanguin, H., Poté, J., Navarro, E., Bernillon, D., Mavingui, P., … Simonet, P. (2008). Antibiotic-resistant soil bacteria in transgenic plant fields. *Proceedings of the National Academy of Sciences of the United States of America*, *105*(10), 3957–3962. doi: 10.1073/pnas.0800072105

Derrien, M., Collado, M. C., Ben-Amor, K., Salminen, S., & de Vos, W. M. (2008). The mucin degrader *Akkermansia muciniphila* is an abundant resident of the human intestinal tract. *Applied and Environmental Microbiology*, *74*(5), 1646–1648. doi: 10.1128/AEM.01226-07

Derrien, M., Vaughan, E. E., Plugge, C. M., & de Vos, W. M. (2004). *Akkermansia muciniphila* gen. Nov., sp. Nov., a human intestinal mucin-degrading bacterium. *International Journal of Systematic and Evolutionary Microbiology*, *54*(5), 1469–1476. doi: 10.1099/ijs.0.02873-0

Desai, M. S., Seekatz, A. M., Koropatkin, N. M., Kamada, N., Hickey, C. A., Wolter, M., … Martens, E. C. (2016). A dietary fiber-deprived gut microbiota degrades the colonic mucus barrier and enhances pathogen susceptibility. *Cell*, *167*(5), 1339–1353.e21. doi: 10.1016/j.cell.2016.10.043

Donovan, J., & Brown, P. (2005). Euthanasia. *Current Protocols in Neuroscience*, *33*, A.4H.1–A.4H.4. doi: 10.1002/0471142301.nsa04hs33

Eberl, C., Ring, D., Münch, P. C., Beutler, M., Basic, M., Slack, E. C., … Stecher, B. (2020). Reproducible colonization of germ-free mice with the oligo-mouse-microbiota in different animal facilities. *Frontiers in Microbiology*, *10*, 2999. doi: 10.3389/fmicb.2019.02999

Ebrahimzadeh Leylabadlo, H., Sanaie, S., Sadeghpour Heravi, F., Ahmadian, Z., & Ghotaslou, R. (2020). From role of gut microbiota to microbial-based therapies in type 2-diabetes. *Infection, Genetics and Evolution*, *81*, 104268. doi: 10.1016/j.meegid.2020.104268

Elzinga, J., van der Oost, J., de Vos, W. M., & Smidt, H. (2019). The use of defined microbial communities to model host-microbe interactions in the human gut. *Microbiology and Molecular Biology Reviews*, *83*(2), e00054–18. doi: 10.1128/MMBR.00054-18

Faith, J. J., Guruge, J. L., Charbonneau, M., Subramanian, S., Seedorf, H., Goodman, A. L., … Gordon, J. I. (2013). The long-term stability of the human gut microbiota. *Science*, *341*(6141), 1237439. doi: 10.1126/science.1237439

Falony, G., Joossens, M., Vieira-Silva, S., Wang, J., Darzi, Y., Faust, K., … Raes, J. (2016). Population-level analysis of gut microbiome variation. *Science*, *352*(6285), 560–564. doi: 10.1126/science.aad3503

Fischer, F., Romero, R., Hellhund, A., Linne, U., Bertrams, W., Pinkenburg, O., … Steinhoff, U. (2020). Dietary cellulose induces anti-inflammatory immunity and transcriptional programs via maturation of the intestinal microbiota. *Gut Microbes*, *12*(1), 1829962. doi: 10.1080/19490976.2020.1829962

Garzetti, D., Brugiroux, S., Bunk, B., Pukall, R., McCoy, K. D., Macpherson, A. J., & Stecher, B. (2017). High-quality whole-genome sequences of the oligo-mouse-microbiota bacterial Community. *Genome Announcements*, *5*(42), e00758–17. doi: 10.1128/genomeA.00758-17

Herp, S., Brugiroux, S., Garzetti, D., Ring, D., Jochum, L. M., Beutler, M., … Stecher, B. (2019). *Mucispirillum schaedleri* antagonizes salmonella virulence to protect mice against colitis. *Cell Host & Microbe*, *25*(5), 681–694.e8. doi: 10.1016/j.chom.2019.03.004

Kittler, J., Illingworth, J., & Föglein, J. (1985). Threshold selection based on a simple image statistic. *Computer Vision, Graphics, and Image Processing*, *30*(2), 125–147. doi: 10.1016/0734-189X(85)90093-3

Kuczma, M. P., Szurek, E. A., Cebula, A., Chassaing, B., Jung, Y.-J., Kang, S.-M., … Ignatowicz, L. (2020). Commensal epitopes drive differentiation of colonic T_{regs}. *Science Advances*, *6*(16), eaaz3186. doi: 10.1126/sciadv.aaz3186

Li, H., Limenitakis, J. P., Fuhrer, T., Geuking, M. B., Lawson, M. A., Wyss, M., … Macpherson, A. J. (2015). The outer mucus layer hosts a distinct intestinal microbial niche. *Nature Communications*, *6*, 8292. doi: 10.1038/ncomms9292

Lourenço, M., Chaffringeon, L., Lamy-Besnier, Q., Pédron, T., Campagne, P., Eberl, C., … De Sordi, L. (2020). The spatial heterogeneity of the gut limits predation and fosters coexistence of bacteria and bacteriophages. *Cell Host & Microbe*, *28*(3), 390–401.e5. doi: 10.1016/j.chom.2020.06.002

Lozupone, C. A., Stombaugh, J. I., Gordon, J. I., Jansson, J. K., & Knight, R. (2012). Diversity, stability and resilience of the human gut microbiota. *Nature*, *489*(7415), 220–230. doi: 10.1038/nature11550

Ludwig, W., Strunk, O., Westram, R., Richter, L., Meier, H., Buchner, Y. A., … Schleifer, K.-H. (2004). ARB: A software environment for sequence data. *Nucleic Acids Research*, *32*(4), 1363–1371. doi: 10.1093/nar/gkh293

Macpherson, A. J., & McCoy, K. D. (2015). Standardised animal models of host microbial mutualism. *Mucosal Immunology*, *8*(3), 476–486. doi: 10.1038/mi.2014.113

Manz, W., Amann, R., Ludwig, W., Wagner, M., & Schleifer, K.-H. (1992). Phylogenetic oligodeoxynucleotide probes for the major subclasses of proteobacteria: Problems and solutions. *Systematic and Applied Microbiology*, *15*(4), 593–600. doi: 10.1016/S0723-2020(11)80121-9

Marion, S., Desharnais, L., Studer, N., Dong, Y., Notter, M. D., Poudel, S., … Bernier-Latmani, R. (2020). Biogeography of microbial bile acid transformations along the murine gut. *Journal of Lipid Research*, *61*(11), 1450–1463. doi: 10.1194/jlr.RA120001021

Moszak, M., Szulińska, M., & Bogdański, P. (2020). You are what you eat–the relationship between diet, microbiota, and metabolic disorders–a review. *Nutrients*, *12*(4), 1096. doi: 10.3390/nu12041096

Nagao-Kitamoto, H., & Kamada, N. (2017). Host-microbial cross-talk in inflammatory bowel disease. *Immune Network*, *17*(1), 1–12. doi: 10.4110/in.2017.17.1.1

Nakajima, A., Vogelzang, A., Maruya, M., Miyajima, M., Murata, M., Son, A., … Suzuki, K. (2018). IgA regulates the composition and metabolic function of gut microbiota by promoting symbiosis between bacteria. *The Journal of Experimental Medicine*, *215*(8), 2019–2034. doi: 10.1084/jem.20180427

Pereira, F. C., Wasmund, K., Cobankovic, I., Jehmlich, N., Herbold, C. W., Lee, K. S., … Berry, D. (2020). Rational design of a microbial consortium of mucosal sugar utilizers reduces *Clostridiodes difficile* colonization. *Nature Communications*, *11*(1), 5104. doi: 10.1038/s41467-020-18928-1

Quast, C., Pruesse, E., Yilmaz, P., Gerken, J., Schweer, T., Yarza, P., … Glöckner, F. O. (2013). The SILVA ribosomal RNA gene database project: Improved data processing and web-based tools. *Nucleic Acids Research*, *41*, D590–D596. doi: 10.1093/nar/gks1219

Riva, A., Kuzyk, O., Forsberg, E., Siuzdak, G., Pfann, C., Herbold, C., … Berry, D. (2019). A fiber-deprived diet disturbs the fine-scale spatial architecture of the murine colon microbiome. *Nature Communications*, *10*(1), 4366. doi: 10.1038/s41467-019-12413-0

Stecher, B., Barthel, M., Schlumberger, M. C., Haberli, L., Rabsch, W., Kremer, M., & Hardt, W.-D. (2008). Motility allows *S. typhimurium* to benefit from the mucosal defence. *Cellular Microbiology*, *10*(5), 1166–1180. doi: 10.1111/j.1462-5822.2008.01118.x

Stecher, B., Chaffron, S., Käppeli, R., Hapfelmeier, S., Freedrich, S., Weber, T. C., … Hardt, W.-D. (2010). Like will to like: Abundances of closely related species can predict susceptibility to intestinal colonization by pathogenic and commensal bacteria. *PLoS Pathogens*, *6*(1), e1000711. doi: 10.1371/journal.ppat.1000711

Stoecker, K., Dorninger, C., Daims, H., & Wagner, M. (2010). Double labeling of oligonucleotide probes for fluorescence in situ hybridization (DOPE-FISH) improves signal intensity and increases rRNA accessibility. *Applied and Environmental Microbiology*, *76*(3), 922–926. doi: 10.1128/AEM.02456-09

Studer, N., Desharnais, L., Beutler, M., Brugiroux, S., Terrazos, M. A., Menin, L., … Hapfelmeier, S. (2016). Functional intestinal bile acid 7α dehydroxylation by *Clostridium scindens* associated with protection from *Clostridium difficile* infection in a gnotobiotic mouse model. *Frontiers in Cellular and Infection Microbiology*, *6*, 191. doi: 10.3389/fcimb.2016.00191

Swidsinski, A., Loening-Baucke, V., Vaneechoutte, M., & Doerffel, Y. (2008). Active Crohn's disease and ulcerative colitis can be specifically diagnosed and monitored based on the biostructure of the fecal flora. *Inflammatory Bowel Diseases*, *14*(2), 147–161. doi: 10.1002/ibd.20330

Tropini, C., Earle, K. A., Huang, K. C., & Sonnenburg, J. L. (2017). The gut microbiome: connecting spatial organization to function. *Cell Host & Microbe*, *21*(4), 433–442. doi: 10.1016/j.chom.2017.03.010

van Tilburg Bernardes, E., Pettersen, V. K., Gutierrez, M. W., Laforest-Lapointe, I., Jendzjowsky, N. G., Cavin, J.-B., … Arrieta, M.-C. (2020). Intestinal fungi are causally implicated in microbiome assembly and immune development in mice. *Nature Communications*, *11*(1), 2577. doi: 10.1038/s41467-020-16431-1

Wotzka, S. Y., Kreuzer, M., Maier, L., Arnoldini, M., Nguyen, B. D., Brachmann, A. O., … Hardt, W.-D. (2019). *Escherichia coli* limits *Salmonella typhimurium* infections after diet shifts and fat-mediated microbiota perturbation

in mice. *Nature Microbiology*, *4*(12), 2164–2174. doi: 10.1038/s41564-019-0568-5

Wyss, M., Brown, K., Thomson, C. A., Koegler, M., Terra, F., Fan, V., … McCoy, K. D. (2020). Using precisely defined in vivo microbiotas to understand microbial regulation of IgE. *Frontiers in Immunology*, *10*, 3107. doi: 10.3389/fimmu.2019.03107

Zhao, L., Zhang, X., Zuo, T., & Yu, J. (2017). The composition of colonic commensal bacteria according to anatomical localization in colorectal cancer. *Engineering*, *3*(1), 90–97. doi: 10.1016/J.ENG.2017.01.012

Internet Resources

http://www.arb-home.de

ARB software for designing probe sequences in silico; comprises tools for sequence database handling and data analysis (also see Ludwig et al., 2004).

https://dome.csb.univie.ac.at/daime

Digital Image Analysis in Microbial Ecology (DAIME), version 2.2; allows bacterial biovolume localization and quantification and comprises various other tools to analyze and visualize 2D and 3D microscopy datasets (also see Daims et al., 2006).